RSC Advances

This is an *Accepted Manuscript*, which has been through the Royal Society of Chemistry peer review process and has been accepted for publication.

Accepted Manuscripts are published online shortly after acceptance, before technical editing, formatting and proof reading. Using this free service, authors can make their results available to the community, in citable form, before we publish the edited article. This *Accepted Manuscript* will be replaced by the edited, formatted and paginated article as soon as this is available.

You can find more information about *Accepted Manuscripts* in the Information for Authors.

Please note that technical editing may introduce minor changes to the text and/or graphics, which may alter content. The journal's standard Terms & Conditions and the Ethical guidelines still apply. In no event shall the Royal Society of Chemistry be held responsible for any errors or omissions in this *Accepted Manuscript* or any consequences arising from the use of any information it contains.

ROYAL SOCIETY OF CHEMISTRY

www.rsc.org/advances

Journal Name

RSCPublishing

ARTICLE

In situ growth of ZnO nanorod arrays on cotton cloth for the removal of uranium (VI)

Cite this: DOI: 10.1039/xoxxoooooox

Lei Zhang, [a] Liang Zhang, [a] Tianhao Wu, [c] Xiaoyan Jing, [a] Rumin Li, [a] Jingyuan Liu, [a] Qi Liu *[a] and Jun Wang*[ab]

Received ooth January 2012,
Accepted ooth January 2012

DOI: 10.1039/xoxxoooooox

www.rsc.org/

In situ growth of ZnO nanorod arrays on cotton cloth (ZnO/CC) was proposed to remove uranium (VI) from aqueous solution. The as-prepared adsorbent is easy separation from the reaction medium after adsorption. The effect factors for uranium adsorption, such as solution pH, initial U (VI) concentration, contact time, and temperature have been systematically investigated. The maximum adsorption capacity of uranium (VI) which was calculated by the Langmuir model at pH=5.0 and T=298 K is 431.03 mg g^{-1}, exhibiting its excellent uranium adsorption properties. It was observed that the kinetic data fit well to the pseudo-second-order kinetic model indicating that the rate-limiting step of adsorption process is chemical adsorption. Moreover, thermodynamic parameters [ΔH°=20.26 kJ mol^{-1} ΔG°=-5.66 kJ mol^{-1} (298 K) ΔS°=86.98 J $mol^{-1}K^{-1}$] reveal that the uranium adsorption is endothermic and spontaneous. Therefore, the ZnO/CC is a potential adsorbent for recovery of uranium (VI) from aqueous solution.

1. Introduction

Recently, significant attentions have been focus on nuclear power industry due to the depletion of fossil fuels.[1-3] However, the depletable conventional uranium resources can only last for about decades.[4] Considering that the uranium mining and hydrometallurgy process usually causes serious water pollution,[5-9] it is necessary to extract uranium from industrial nuclear waste water which contains abundant and dissolved uranium (VI) for the sustainable development of nuclear power.[2,10]

Many techniques, such as ion exchange, reverse osmosis, co-precipitation, have been developed to remove uranium from aqueous medium.[11-13] Compared with the methods above, uranium adsorption is relatively efficient and low cost.[14,15] Therefore, different types of adsorbent have been prepared for recovery of uranium (VI) from aqueous solution.[16] Nair et al have used SiO_2, Al_2O_3, TiO_2 and FeOOH to adsorb uranyl and arsenate.[17] Xu et al have synthesized amidoximated chitosan-grafted polyacrylonitrile for uranium (VI) adsorption.[18] Gu et al have prepared graphene oxide-carbon nanotubes hybrid aerogels for removal of uranium (VI).[19] Among this adsorbents, metal oxides, such as manganese dioxide, titanium dioxide and zinc oxide, have received enormous attention due to its availability, thermostability and environmental friendliness.[10,20]

As a multifunctional and environmental friendly material, ZnO has been used for uranium (VI) adsorption.[21] Recently, Kaynar et al have prepared nanoporous ZnO for removal of uranium.[22] Hallaji et al have synthesized a novel PVA/ZnO nanofiber adsorbent to remove U (VI), Cu (II) and Ni (II) from aqueous solution.[23] Although the as-prepared ZnO have shown large adsorption capacity for uranium due to large specific surface area and rich active surface sites.[21] However, as a kind of superfine powder, ZnO is difficult to be separated from solution. Therefore, further treatment for adsorbent should be considered. An effective method to solve this problem is finding a carrier for ZnO.[24] As a kind of substrate materials, cotton cloth is cost-effective and environmental-friendly. The hydroxyl on the surface of cotton fibers is facile to ZnO seeded sol loading on the substrate. In addition, the flexible cotton cloth substrate is also convenient to recycle after adsorption. Therefore, cotton cloth could serve as the substrate material for ZnO powder.

As a proof-of-concept, ZnO nanorod arrays have been fabricated on cotton cloth by a two-step method: cotton cloth modified with ZnO seeded sol and in situ growth of ZnO nanorod arrays on cotton cloth. Chemical components and structure of ZnO/CC are characterized by XRD, SEM and TEM methods. The process of the obtained ZnO/CC for uranium (VI) adsorption on aqueous solution was also fully researched. The results show that the as-prepared adsorbent not only possesses high adsorption capacity for uranium (VI) but also can be easily separated from aqueous system. Such high efficient and environmental friendly ZnO/CC adsorbent will further promote uranium adsorption for practical application.

2. Experimental

RSC Advances Accepted Manuscript

2.1 Chemicals

$Zn(CH_3COO)_2·4H_2O$, $Zn(NO_3)_2·6H_2O$, $UO_2(NO_3)_2·6H_2O$, NaOH, hexamethylenetetramine and ethanol were purchased from Tianjin Kermel Chemical Reagents Company. Cotton cloth (medical) was obtained from local market. Stock solutions of uranium (VI) were prepared by dissolving uranyl nitrate in deionized water at the desired initial concentrations. All chemical reagents were used without further purification.

2.2 Preparation of ZnO/CC

Cotton cloth modified with ZnO seeded sol. 0.120 g NaOH and 0.114 g $Zn(CH_3COO)_2·4H_2O$ were dispersed in 100 and 75 mL ethanol, respectively. The above solutions were mixed to obtain a ZnO seeded sol after stirring for 4 h at 60 ℃. Then, the cotton cloth was immersed in the ZnO seeded sol for 5min. After that, cotton cloth was taken out and annealed at 150 ℃.

In situ growth of ZnO nanorod arrays on cotton cloth.[25] 3.000 g $Zn(NO_3)_2·6H_2O$ and 1.400 g hexamethylenetetramine were dissolved in 100 mL deionized water. Then, 0.500 g modified cotton cloth was added to the above solution to form a homogeneous mixture. After that, the mixture were transferred into a Teflon-lined autoclave, sealed and heated for 4 h at 95 ℃. After cooling to room temperature, the product was separated by filter, washed with deionized water andabsolute alcohol several times, and then dried in at 50 ℃.

2.3 Adsorption experiments

Uranium adsorption experiments were carried out the following procedure: a given dose of ZnO/CC was shaken together with the 20 mL uranium (VI) solution in a conical flask. The conical flask was placed in a thermostatic water shaker at speed of 150 rpm. In this process, the experimental parameters of adsorption were changed, including solution concentration, solution pH, adsorption time and temperature. The pH value of working solution was adjusted with HNO_3 or NaOH solution. After the adsorption reached equilibrium, the ^{VI}U-ZnO/CC was separated out with tweezers. The adsorption capacity (Q_e) was calculated using the following equation:[26]

$$Q_e = \frac{(C_0 - C_e)V}{m} \quad (1)$$

where C_0 (mg L^{-1}) and C_e (mg L^{-1}) are initial concentration and equilibrium concentration, respectively. m (g) is the weight of ZnO/CC, V (L) is the volume of the solution. The adsorption removal efficiency (η) and distribution coefficient (K_D) were obtained according to following equations:[14]

$$\eta = \frac{C_0 - C_e}{C_0} \times 100\% \quad (2)$$

$$K_D = \frac{C_0 - C_e}{C_e} \times \frac{V}{m} \quad (3)$$

2.4 Characterization

The structures of ZnO/CC and cotton cloth were analyzed by a Rigaku X-ray power diffractometer with Cu-Kα radiation (40kV, 150mA). The morphology of ZnO/CC was characterized using SEM and TEM. The SEM images were recorded on a JEOL JSM-6480 with an energy-dispersive X-ray spectrum. The TEM images were performed on a Tecnai G^2 20 STWIN with an accelerating voltage of 200kV. The uranium (VI) concentration was analyzed using WGJ-III Trace Uranium Analyzer. The concentration of zinc (II) was analyzed by ICP.

3. Results and discussions

3.1 Characterization of samples

The XRD patterns of cotton cloth and ZnO/CC are shown in Fig.1. The diffraction peaks are caused by cellulose crystal at 15°, 17° and 22°, respectively. All strong peaks (100), (002), (101), (110), (103), (112), (201) and (202) can be identified and indexed to ZnO (JCPDS. 36-1451).[27,28] The sharp diffraction peaks of ZnO/CC indicate that the crystallized ZnO was successfully fabricated on the fibers of cotton cloth. From Fig. 2a-b, it also can be observed that ZnO nanorod arrays were grown on the modified cotton cloth.

Fig.3a-c show the SEM images of cotton cloth, modified cotton cloth and ZnO/CC, respectively. The ZnO seeded sol was coated on the fibers of cotton cloth (Fig. 3 a and b). Moreover, ZnO nanorod arrays were densely and uniformly

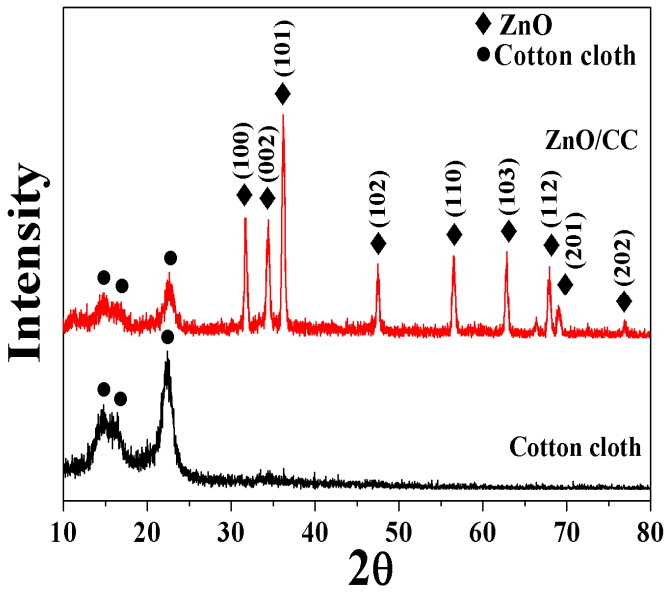

Fig.1 XRD patterns of ZnO/CC and cotton cloth.

RSC Advances Accepted Manuscript

This journal is © The Royal Society of Chemistry 2012

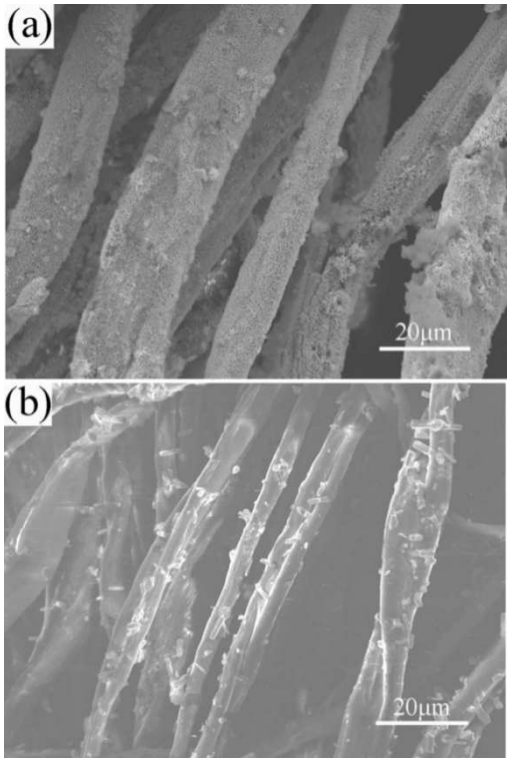

Fig.2 (a) SEM image of an as-prepared ZnO/CC using the modified cotton cloth; (b) SEM image of an as-prepared ZnO/CC using the unmodified cotton cloth.

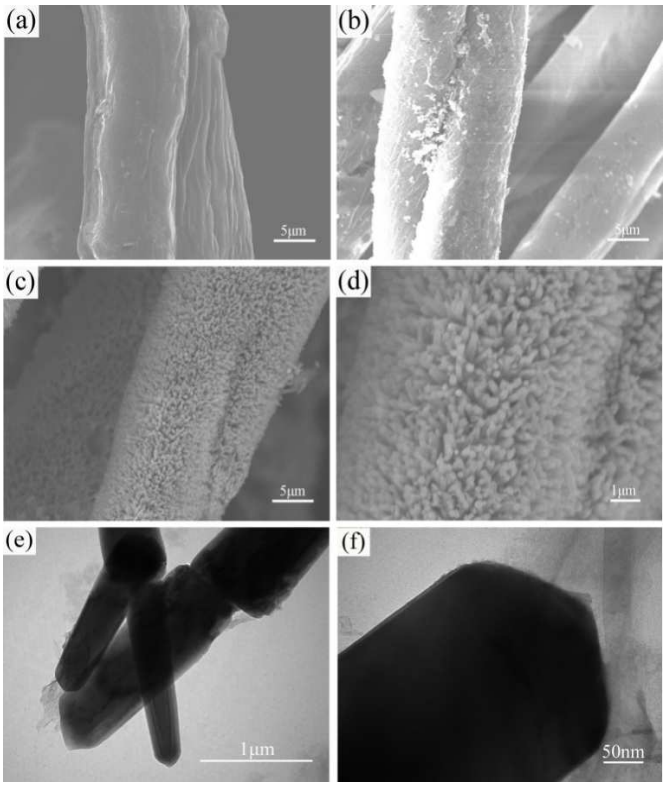

Fig.3 SEM images of cotton cloth (a), cotton cloth modified with ZnO seeded sol (b), cotton cloth in situ grown ZnO rod arrays (c) and (d); TEM images of rod ZnO (e) and (f).

covered on fibers of cotton cloth (Fig.3c-d). Further detailed structural analysis of ZnO nanorod was carried out by TEM. Fig.3e shows that the diameter of ZnO nanorod is different and the phenomenon of overlapping growth was manifested. The rod diameter of ZnO can be evaluated to be 150-200 nm. When the TEM was magnified, the as-prepared ZnO shows inerratic columnar structure (Fig.3f). Fig.4 a-b show the actual object of ZnO/CC adsorbed beforeand after uranium (VI). From Fig. 4b, it is evident that the white ZnO/CC changed to yellow after adsorbing uranium (VI), indicating the good result of adsorption toward uranium (VI). In order to investigate the adhesion of ZnO nanorods on the cotton fiber, ZnO/CC was treated by ultrasound for 10 min. As shown in Table S1, the weight loss for ZnO/CC after ultrasound is about 2 mg, revealing that the good adhesion of ZnO nanorods on cotton fibers.

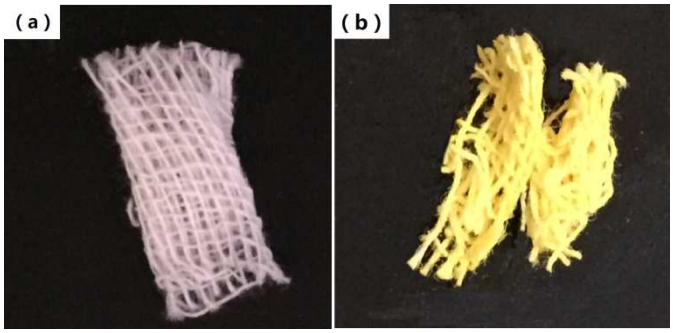

Fig.4 Actual object of ZnO/CC before (a) and after (b) adsorbed uranium (VI).

3.2 Effect of solution pH

The pH of a solution is an important parameter for adsorption because it can influence chemical property of adsorbent and hydrolysis species of uranium (VI).[29] In general, adsorbents have excellent adsorption capacity at certain value of pH. The

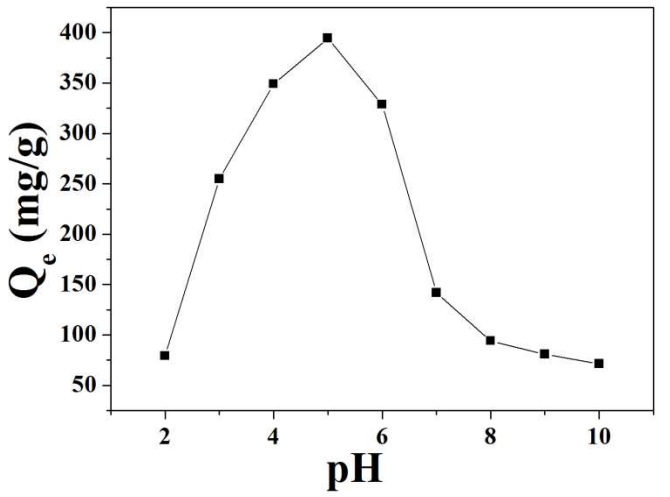

Fig.5 Effect of pH on the adsorption of uranium (VI), C_0=200.00 mg L^{-1}, t=2 h, T=298 K.

RSC Advances Accepted Manuscript

adsorption of uranium (VI) on ZnO/CC was carried out at different pH values from 2.0 to 10.0. The adsorption time is 2 h and the concentration of uranium (VI) solution is 200.00 mg L^{-1}. It can be seen that the adsorption capacity reaches to the maximum value when the pH is 5.0 (Fig.5). When the pH of solution is low, hydrogen ions can compete with uranyl ions to adsorb on ZnO/CC. In addition, the ZnO/CC can be damaged by hydrogen ions.[30,31] Along with the increase of pH, a lot of Zn^{2+} which can exchange with uranyl ions attached to surface of ZnO nanorods, resulting in an increased adsorption capacity. When the pH is higher than 6.0, hydrolyzed uranyl ion cannot be adsorbed on surface of ZnO/CC. Based on the above analysis, the optimal pH is 5.0.

3.3 Effect of adsorbent dose

The effect of the uranium removal on the dosage of ZnO/CC was carried out by using different adsorbent doses from 0.002 to 0.012 g at fixed initial concentration of uranium (VI). The working initial concentration of uranium (VI) was 200.00 mg L^{-1}. Fig.6 shows the removal efficiency increased with the increasing amount of adsorbent clearly. The more availability adsorption sites were involved in adsorption of uranium (VI) at higher dosage. When 0.010g adsorbent was used, the maximum removal efficiency was attained. When the amount of adsorbent exceeded 0.010 g, the constant of the removal efficiency and the decrease of the adsorption capacity indicate that the adsorption remained unsaturated state. From an economical point of view, 0.010 g of ZnO/CC is considered as an optimum dose.

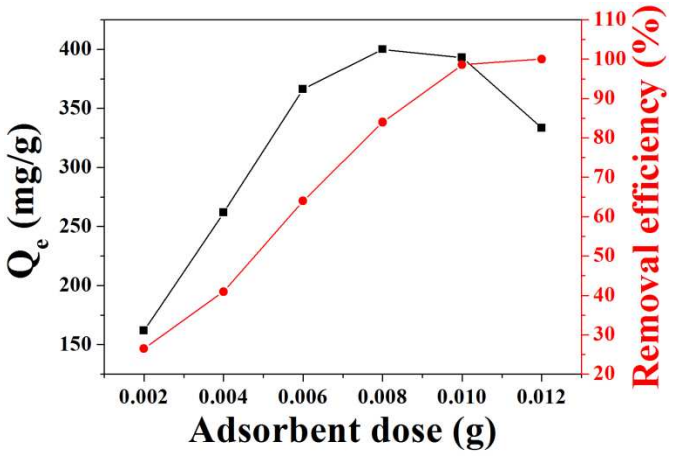

Fig.6 Effect of amount of adsorbent on the adsorption of uranium (VI), C_0=200.00 mg L^{-1}, pH=5.0, t=4 h, T=298 K.

3.4 Effect of initial concentration of uranium (VI) and adsorption isotherms

The study of uranium (VI) concentration influenced on adsorption was carried out using different initial uranium (VI) concentrations which ranged from 100.00 to 350.00 mg L^{-1}.

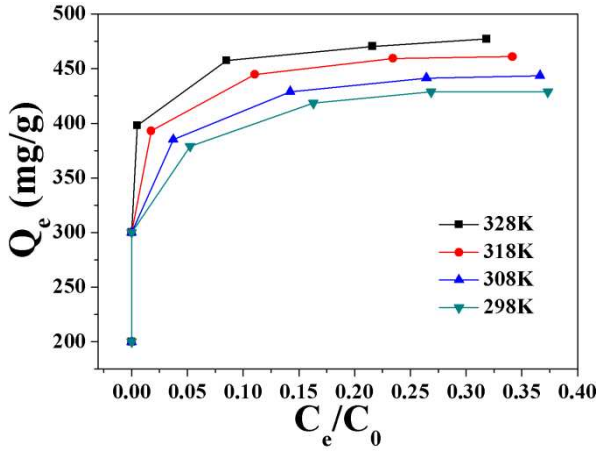

Fig.7 Isotherm of uranium (VI) adsorption onto ZnO/CC, pH=5.0, t=4 h.

The results in Fig. 7 express that adsorption capacity of uranium (VI) increases with the increasing concentration of uranium (VI). This is due to obtaining a high driving force which overcomes transfer resistance, when the concentration of uranium (VI) increases.[32] Moreover, the equilibrium adsorption capacity increases as temperature rose. Furthermore, the adsorption experiments in uranium (VI) solutions with pure cotton cloth and ZnO/CC grown without seeding were carried out at 298 K. (Table S2)

The adsorption data were analyzed using Langmuir and Freundlich isotherms. The Langmuir isotherm based on monolayer adsorption can be represented by Eq. 4.[33]

$$\frac{C_e}{Q_e} = \frac{1}{K_L Q_m} + \frac{C_e}{Q_m} \quad (4)$$

where K_L is an equilibrium constant (L mg^{-1}), Q_e and Q_m are equilibrium adsorption capacity and maximum adsorption capacity (mg g^{-1}), respectively. As an empirical equation Freundlich isotherm is applicable to heterogeneous surfaces. The empirical equation of Freundlich isotherm can be expressed as follow:

$$lnQ_e = lnK_F + \frac{1}{n} lnC_e \quad (5)$$

where K_F is Freundlich constant, n is adsorption intensity. The linear plots of Langmuir and Freundlich equations representing uranium (VI) adsorption are illustrated in Fig.8. The corresponding parameters of Langmuir and Freundlich equations were calculated in Table S3. Comparing the two correlating coefficients (R^2) of isotherms, it is confirmed that the Langmuir isotherm is more suitable to characterize the behavior of uranium (VI) adsorption on ZnO/CC. The Langmuir constant (K_L) and the maximum adsorption capacity

RSC Advances Accepted Manuscript

This journal is © The Royal Society of Chemistry 2012

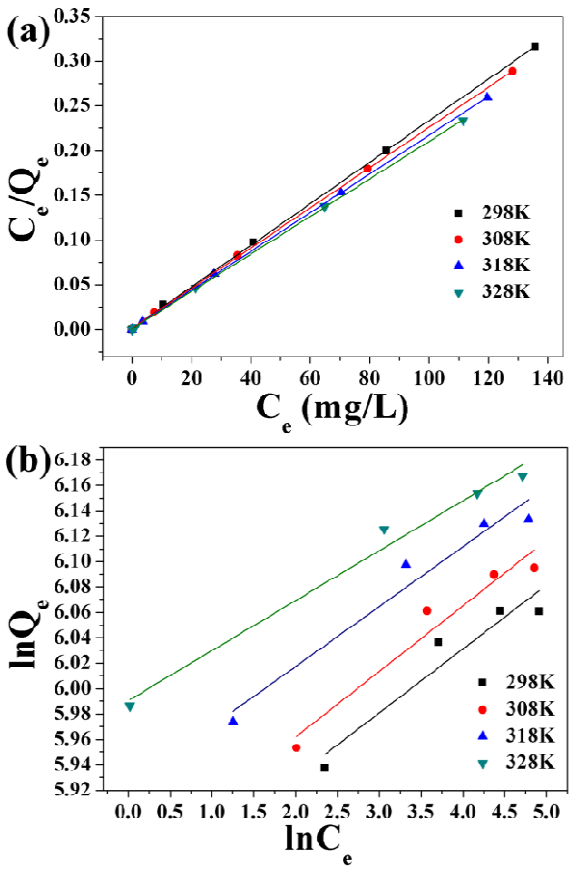

Fig.8 Langmuir (a) and Freundlich (b) isotherms of uranium (VI) on ZnO/CC.

(Q_m) were evaluated from the intercept and slope of the Langmuir plots. The values of K_L show a strong bonding energy between ZnO/CC and uranium (VI). The maximum adsorption capacity reaches 431.03 mg g^{-1}, exhibiting its excellent performance of uranium adsorption at room temperature (298 K). All the parameters were obtained in the initial concentration from 100.00 to 350.00 mg L^{-1} and 10 mg of adsorbent in 20 mL of adsoebate at pH 5.0 for 4 h.

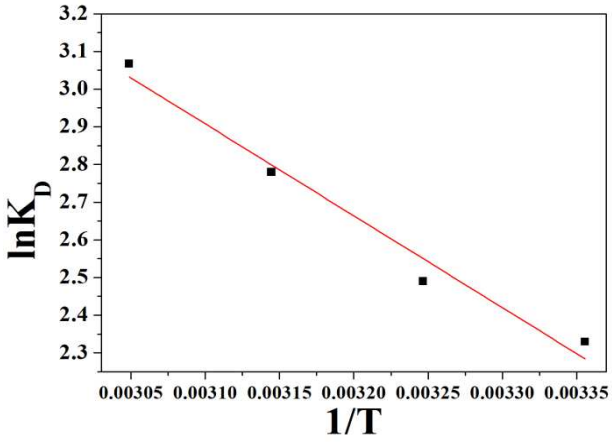

Fig.9 Relationship curve between lnKD and 1/T.

3.5 Effect of temperature and thermodynamic study

As can be seen from Fig.7, the adsorption of uranium (VI) is favored with an increased temperature from 298 to 328 K. The corresponding adsorption capacity of uranium (VI) is increased from 428.76 to 470.44 mg g^{-1}. This can be explained that the more adsorption sites were activated with the increase of temperature. In order to understand the nature and thermodynamic feasibility of the adsorption process, the standard free energy (ΔG^0), standard enthalpy (ΔH^0) and standard entropy (ΔS^0) are calculated from adsorption data at different temperatures. The three thermodynamic parameters are calculated using the following equations:[34]

$$\ln K_D = -\frac{\Delta H^0}{RT} + \frac{\Delta S^0}{R} \quad (6)$$

$$\Delta G^0 = \Delta H^0 - T\Delta S^0 \quad (7)$$

where K_D is the distribution coefficient (mL g^{-1}), R is the ideal gas constant (8.314 kJ $mol^{-1}K^{-1}$), T is the temperature (K). The ΔH^0 and ΔS^0 were determined from the slope and intercept of lnK_D versus T^{-1}, respectively (Fig. 9). According to Table S4, the value of ΔH^0 is positive, demonstrating that the process of uranium adsorption on ZnO/CC is endothermic. The negative values of ΔG^0 confirm that the process is spontaneous nature. The positive value of ΔS^0 suggests an increase of randomness at the solid-liquid interface. And it also indicates that the adsorption of uranium (VI) on ZnO/CC is in a range of the dissociative mechanism.[35] Through the above analysis, the increase of temperature is conducive to adsorption of uranium (VI) on ZnO/CC.

3.6 Effect of contact time and adsorption dynamics

Fig.10 shows the amount of uranyl ion adsorbed on ZnO/CC as a function of the contact time at a fixed temperature. It is clear that the adsorption capacity increases with the increase of contact time, and the adsorption equilibrium is established after 30 min. The rate of adsorption increases rapidly during the first 10 min due to the strong interaction between ZnO/CC and uranium (VI). Then the rate of adsorption gradually reduces with the decrease of active sites. To investigate the controlling mechanism of the adsorption process, the adsorption data were analyzed using pseudo-first-order and pseudo-second-order kinetic equations. The pseudo-first-order kinetic and pseudo-second-order models are given as:[36]

$$\ln(Q_e - Q_t) = \ln Q_e - k_1 t \quad (8)$$

$$\frac{t}{Q_t} = \frac{1}{k_2 Q_e^2} + \frac{1}{Q_e} t \quad (9)$$

where Q_e and Q_t (mg g^{-1}) are adsorption capacity at equilibrium and at time, respectively. k_1 (min^{-1}) is the rate constant of the

RSC Advances Accepted Manuscript

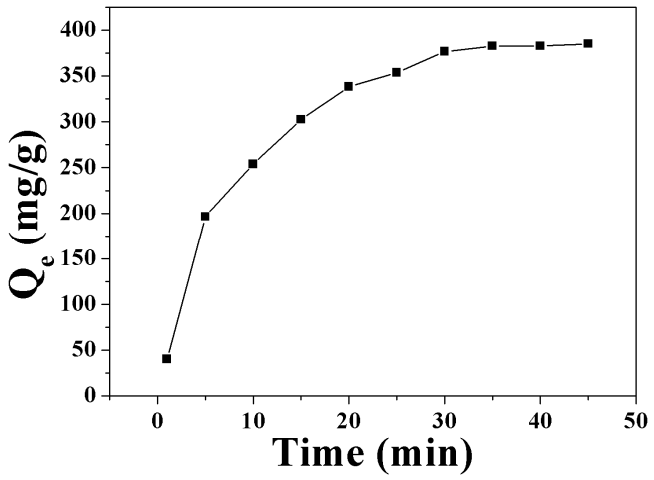

Fig.10 Effect of contact time on uranium (VI) adsorption, m=0.010 g, C_0=200.00 mg L^{-1}, T=298 K.

pseudo-first-order kinetic equation, k_2 (g mg^{-1} min^{-1}) is the rate constant of the pseudo-second-order kinetic equation.

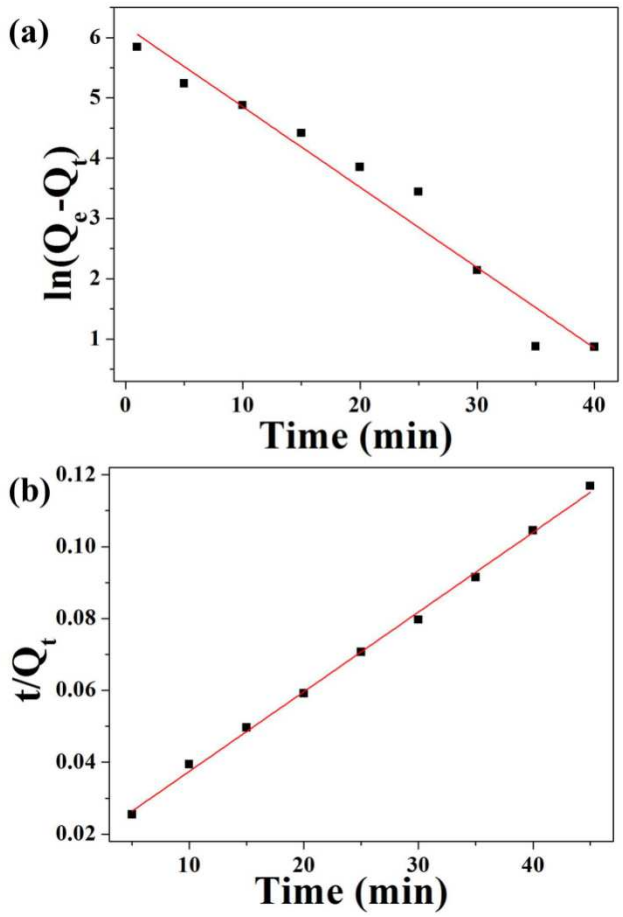

Fig.11 Pseudo-first-order (a), pseudo-second-order (b), plot for the adsorption of uranium (VI) by ZnO/CC.

The values of Q_e, k_2 can be obtained by plotting t/Q_t vs. t (Fig. 11b), these are presented in Table S5. According to correlation coefficients (0.99>0.91), the adsorption of uranium (VI) on ZnO/CC follows the pseudo-second-order model better than the pseudo-first-order model. The pseudo-second-order kinetic model assumes that the rate-limiting step may be chemical adsorption.[37] It is more likely to predict that the mechanism of the adsorption process may be ion exchange.

3.7 Comparison of uranium (VI) adsorption capacity of ZnO/CC with other adsorbents

The adsorption capacities of different uranium adsorbents reported in literatures are listed in Table S6.[38-44] The data reveal that adsorption capacity of ZnO/CC (431.03 mg g^{-1}) is superior to some materials adsorbed uranium (VI). In addition, the nanoporous ZnO prepared by microwave-assisted combustion synthesis possesses have a higher adsorption capacity. However, the ZnO/CC is a more suitable material for uranium (VI) sorption because it is easily separated from solution.

3.8 Adsorption mechanism and strategy for enrichment of uranium (VI)

The coordination mechanism of interaction between ZnO/CC and uranium (VI) was speculated in Scheme 1. Reaction mechanism can be described as follows: ① H^+ from the solution reacts with ZnO, generating $ZnOH^+$ and $[Zn_2O]^{2+}$ covering on the surface of the rod at pH 5.0. ② UO_2^{2+} subsequently can replace Zn^{2+} and H^+ dispersing in the solution. The variation of pH (from 5.0 to 4.7) and occurrence of Zn^{2+} from ICP data (Table S7) indirectly prove speculation.

It is an important factor to desorb and enrich uranyl from the adsorbent. To save the costs and improve the utilization rate of raw materials, adsorbent-ZnO/CC was re-prepared. And the uranyl was desorbed and enriched, simultaneously. As shown in Scheme 2, a novel strategy was devised for the enrichment of the uranyl and re-preparation of the adsorbent. Firstly, ZnO/CC adsorbed uranium (VI) was immersed into dilute nitric acid solution to produce zinc nitrate and uranyl nitrate. Then, excessive amounts of the $NH_3 \cdot H_2O$ were added to the above solution. White and yellow precipitations were present in

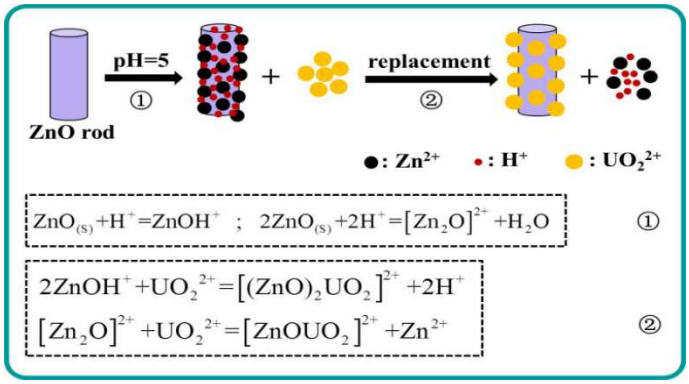

Scheme1. Proposed mechanism of the adsorption of uranium (VI).

RSC Advances Accepted Manuscript

This journal is © The Royal Society of Chemistry 2012

solution. As the concentration of ammonium hydroxide increased, the white precipitation gradually dissolved by eqn as follow:

$$Zn(NO_3)_2+2NH_3\cdot H_2O=Zn(OH)_2\downarrow+2NH_4NO_3 \quad (10)$$

$$2UO_2(NO_3)_2+6NH_3\cdot H_2O=(NH_4)_2U_2O_7\downarrow +4NH_4NO_3+3H_2O \quad (11)$$

$$Zn(OH)_2+2NH_3\cdot H_2O+2NH_4NO_3=[Zn(NH_3)_4](NO_3)_2 +4H_2O \quad (12)$$

According to the ① in Scheme 2, the supernatant filtered out yellow precipitation was carried out by drying treatment at 50 ℃. The XRD pattern (Scheme 2c) confirms that the white powder is composed of zinc oxide and ammonium nitrate. Scheme 2d is SEM image of the white powder. The ZnO was obtained through calcining the white powder at 500 ℃ (②). The XRD pattern and SEM image (Scheme 2e-f) also confirm that the white powder decomposed into ZnO. Scheme 2a and b are XRD pattern and SEM image of the $(NH_4)_2U_2O_7$, respectively. Finally, the obtained ZnO, a certain concentration of nitric acid, new modified cotton cloth and a certain amount of hexamethylenetetramine were transferred into a Teflon-lined autoclave for the regeneration of the ZnO/CC adsorbent. Moreover, the regenerated ZnO/CC adsorbent sustained excellent adsorption ability after three cycles (Fig. S2), indicating that the as-prepared ZnO/CC adsorbent is reusable.

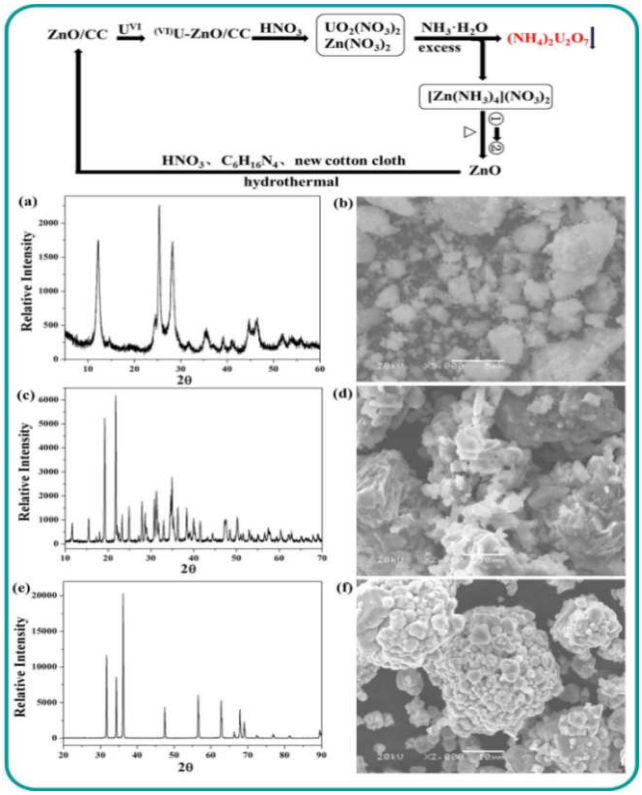

Scheme 2 Design for enrichment of uranyl and recycling of adsorbent; (a) and (b) are XRD pattern and SEM image of the $(NH4)_2U_2O_7$, respectively; (c) and (d) are XRD pattern and SEM image of the product by drying treatment at 50 ℃,respectively; (e) and (f) are XRD pattern and SEM image of the product (ZnO) by follow-up drying treatment at 500 ℃, respectively.

4. Conclusions

In summary, as a cost-effective, nontoxic and environmentally friendly material, the as-prepared ZnO/CC shows significant uranium (VI) removal efficiency. Effects of uranium (VI) concentration, adsorbent dosage, solution pH, contact time and temperature on the adsorption properties for uranium (VI) were fully researched. The results reveal that the maximum uranium adsorption capacity of ZnO/CC is 431.03 mg g^{-1} and the adsorption equilibrium is established after 30 min, showing its high efficiency. Furthermore, the enrichment of uranyl process and the reuse of ZnO/CC adsorbent process have been simultaneously performed via a novel strategy. Such high efficient and environmental friendly ZnO/CC adsorbent will further promote uranium adsorption for practical application.

Acknowledgements

This work was supported by Heilongjiang Province Natural Science Funds for Distinguished Young Scholar (JC201404), Special Innovation Talents of Harbin Science and Technology for Distinguished Young Scholar (2014RFYXJ005), Fundamental Research Funds of the Central University (HEUCFZ), NaturalScience Foundation of Heilongjiang Province (B201316), Program of International S&T Cooperation special project (2015DFR50050), Special Innovation Talents of Harbin Scienceand Technology (2014RFQXJ087).

Notes

Supporting Information

Electronic Supplementary Information (ESI) available: details of any supplementary information available should be included here.

Author Information

a Key Laboratory of Superlight Material and Surface Technology,Ministry of Education, Harbin Engineering University, 150001, PR China.

b Institute of Advanced Marine Materials, Harbin Engineering University, 150001, PRChina.

c Fundamental Science on Nuclear Safety and Simulation Technology Laboratory, Harbin Engineering University, 150001, PR China.

* Corresponding author: Tel.: +86 451 8253 3026; fax: +86 451 8253 3026; E-mail: zhqw1888@sohu.com.

References

1. Q. Cao, Y. C. Liu, C. Z. Wang and J. S. Cheng, *J. Hazard. Mater.*, 2013, **263**, 311.
2. Z. Chen, Z. Y. Zhuang, Q. Cao, X. H. Pan, X. Guan and Z. Lin, *ACS Appl. Mater. Interfaces*, 2014, **6**, 1301.

RSC Advances Accepted Manuscript

3. L. Tan, Y. Wang, Q. Liu, J. Wang, X. Jing, L. Liu, J. Liu and D. Song, *Chem. Eng. J.*, 2015, **259**, 752.
4. N. Singh and K. Balasubramanian, *RSC Adv.*, 2014, **4**, 27691.
5. C. X. Liu, J. Y. Shang, H. M. Shan and J. M. Zachara, *Environ. Sci. Technol.*, 2014, **48**, 1745.
6. H. Foerstendorf, N. Jordan and K. Heim, *J. Colloid Interface Sci.*, 2014, **416**, 133.
7. O. A. Elhefnawy, W. I. Zidan, M. M. Abo-Aly, E. M. Bakier and G. A. Elsayed, *J. Radioanal. Nucl. Chem.*, 2014, **299**, 1821.
8. B. Campos, J. Aguilar-Carrillo, M. Algarra, M. A. Goncalves, E. Rodriguez-Castellon, J. da Silva and I. Bobos, *Appl. Clay Sci.*, 2013, **85**, 53.
9. H. J. Zhang, H. L. Liang, Q. D. Chen and X. H. Shen, *J. Radioanal. Nucl. Chem.*, 2013, **298**, 1705.
10. L. Zhang, X. Jing, R. Li, Q. Liu, J. Liu, H. Zhang, S. Hu and J. Wang, *RSC Adv.*, 2015, **5**, 23144.
11. H. Zhang, Q. Liu, J. Wang, J. Liu, H. Yan, X. Jing and B. Zhang, *RSC Adv.*, 2015, **5**, 5904.
12. K. Z. Elwakeel and A. A. Atia, *J. Cleaner Prod.*, 2014, **70**, 292.
13. D. Humelnicu, C. Blegescu and D. Ganju, *J. Radioanal. Nucl. Chem.*, 2014, **299**, 1183.
14. H. Yan, J. Bai, X. Chen, J. Wang, H. Zhang, Q. Liu, M. Zhang and L. Liu, *RSC Adv.*, 2013, **3**, 23278.
15. A. S. Al-Hobaib and A. A. Al-Suhybani, *J. Radioanal. Nucl. Chem.*, 2014, **299**, 559.
16. X. Zhang, J. Wang, R. Li, Q. Liu, L. Li, J. Yu, M. Zhang and L. Liu, *Environ. Sci. Pollut. Res. Int.*, 2013, **20**, 8202.
17. S. Nair, L. Karimzadeh and B. J. Merkel, *Environ. Earth Sci.*, 2014, **72**, 3507.
18. C. Xu, J. Wang, T. Yang, X. Chen, X. Liu and X. Ding, *Carbohydr. Polym.*, 2015, **121**, 79.
19. Z. Gu, Y. Wang, J. Tang, J. Yang, J. Liao, Y. Yang and N. Liu, *J. Radioanal. Nucl. Chem.*, 2015, **303**, 1835.
20. J. Ramkumar, S. Chandramouleeswaran, B. S. Naidu and V. Sudarsan, *J. Radioanal. Nucl. Chem.*, 2013, **298**, 1845.
21. Y. Yang, J. E. Saiers and M. O. Barnett, *Environ. Sci. Technol.*, 2013, **47**, 2661.
22. U. H. Kaynar, M. Ayvacikli, S. C. Kaynar and U. Hicsonmez, *J. Radioanal. Nucl. Chem.*, 2014, **299**, 1469.
23. H. Hallaji, A. R. Keshtkar and M. A. Moosavian, *J. Taiwan Inst. Chem. Eng.*, 2015, **46**, 109.
24. X. Yu, S. Tong, M. Ge, J. Zuo, C. Cao and W. Song, *J. Mater. Chem. A*, 2013, **1**, 959.
25. Z. Zheng, Z. S. Lim, Y. Peng, L. You, L. Chen and J. Wang, *Sci Rep*, 2013, **3**, 2434.
26. J. Yu, Z. Li, Q. Liu, J. Wang, H. Wei, M. Zhang and L. Liu, *RSC Adv.*, 2013, **3**, 6621.
27. W. Ye, X. Xiao-Lang, X. Wei-Yu, W. Zhuang-Bing, L. Liu and Z. Ya-Li, *Acta Physica Sinica*, 2008, **57**, 2582.
28. H. X. Liu, S. M. Zhou, S. Z. Li, Y. Hang, J. Xu, S. L. Gu and R. Zhang, *Acta Physica Sinica*, 2006, **55**, 1398.
29. J. Qian, S. Zhang, Y. Zhou, P. Dong and D. Hua, *RSC Adv.*, 2015, **5**, 4153.
30. L. Li and M. Schuster,*Sci. Total Environ.*, 2014, **472**, 971.
31 N. Odzak, D. Kistler, R. Behra and L. Sigg,*Environ. Pollut.*,2014, **191**, 135.
32. S. Zhang, J. Li, T. Wen, J. Xu and X. Wang, *RSC Adv.*, 2013, **3**, 2754.
33. S. Zhang, W. Xu, M. Zeng, J. Li, J. Li, J. Xu and X. Wang, *J. Mater. Chem. A*, 2013, **1**, 11691.
34. S. Zhang, M. Zeng, J. Li, J. Li, J. Xu and X. Wang, *J. Mater. Chem. A*, 2014, **2**, 4391.
35. Y. Sun, J. Li and X. Wang, *Geochim. Cosmochim. Acta.*, 2014, **140**, 621.
36. Y. Zhao, J. Li, S. Zhang, H. Chen and D. Shao, *RSC Adv.*, 2013, **3**, 18952.
37. X. Tan, X. Ren, J. Li and X. Wang, *RSC Adv.*, 2013, **3**, 19551.
38. S. P. Dubey, A. D. Dwivedi, M. Sillanpaa, Y. N. Kwon and C. Lee, *RSC Adv.*, 2014, **4**, 46114.
39. J. Wei, X. Zhang, Q. Liu, Z. Li, L. Liu and J. Wang, *Chem. Eng. J.*, 2014, **241**, 228.
40. M. Zeng, Y. Huang, S. Zhang, S. Qin, J. Li and J. Xu, *RSC Adv.*, 2014, **4**, 5021.
41. W. Cheng, M. Wang, Z. Yang, Y. Sun and C. Ding, *RSC Adv.*, 2014, **4**, 61919.
42. W. L. Zhang, Z. B. Zhang, X. H. Cao, R. C. Ma and Y. H. Liu, *J. Radioanal. Nucl. Chem.*, 2014, **301**, 197.
43. S. Li, H. Bai, J. Wang, X. Jing, Q. Liu, M. Zhang, R. Chen, L. Liu and C. Jiao, *Chem. Eng. J.*, 2012, **193**, 372.
44. D. Shao, G. Hou, J. Li, T. Wen, X. Ren and X. Wang,*Chem. Eng. J.*,2014, **255**, 604.

RSC Advances Accepted Manuscript

 This journal is © The Royal Society of Chemistry 2012